UNCLASSIFIED

AD 296 216

Reproduced by the

ARMED SERVICES TECHNICAL INFORMATION AGENCY
ARLINGTON HALL STATION
ARLINGTON 12, VIRGINIA

UNCLASSIFIED

63-2-4

Final Engineering Report

Digital Correlator Study

Navy Department Bureau of Ships

UNIVAC

DIVISION OF SPERRY RAND CORPORATION

December 1962

DEPARTMENT OF THE NAVY
BUREAU OF SHIPS
WASHINGTON 25, D. C.

IN REPLY REFER TO
NObsr 87424
Ser 687D3-38

~~Downgraded to ---------------- when enclosure(s) is/are detached~~

13 FEB 1963

Address All Replies to Chief, Bureau of Ships

TO: Director, Armed Services Technical Information Agency, Arlington Hall Station, ~~Arlington 12, Virginia Attention TIPDR~~

VIA:

THE MATERIAL ITEMIZED BELOW, OR ON ATTACHED LIST, IS FORWARDED AS INDICATED:

	Forwarded per your request
X	*For information and retention*
	On loan and to be returned to the Bureau of Ships
	Return of loaned material
	For use in connection with
	Partial fulfillment of order - Balance will be forwarded when available
	SECRET AND TOP SECRET - THE ATTACHED RECEIPT, OPNAV 5511-10 MUST BE SIGNED AND RETURNED TO THE BUREAU OF SHIPS IMMEDIATELY.

Encl:
(1) Two copies of final engineering report DIGITAL CORRELATOR STUDY (UNIVAC) December 1962 Contract NObsr 87424

M. F. Hodges

M. F. HODGES
By direction

NAVSHIPS 4669 (4-56)

Final Engineering Report
for the
Digital Correlator Study

This report covers the period
1 May 1962 to 1 December 1962

UNIVAC
Division of Sperry Rand Corporation
St. Paul, Minnesota

Navy Department Bureau of Ships
Contract ~~Number~~: 87424
Project Serial Number: SF-007-01-01, Task 7131
NObsr-

December 1962

CONTENTS

ABSTRACT

A systems design study of a digital correlator for waveform recognition purposes has produced a design that is practical for hardware implementation of waveform classification as outlined in the original contract. Two approaches to the correlation problem, referred to as the sum-of-products and the least-squared-difference methods, were investigated. With appropriate normalization the sum-of-products method and the least-squared-difference method can both be used for target classification. The latter method has the following advantages over the former:

a) more economical to implement

b) less time required to identify a given return

c) compensation for changes in the noise level and for certain a priori information

d) analytical justification

Comparisons are made of several designs based upon the different parameters.

Because of the uniqueness of the method proposed for classification, and the uncertainty of the data available in the sonar returns, a simulation study using recorded sonar returns is recommended. The simulation study will determine the validity and accuracy of the correlation process. It also will aid in the selection of various parameters that will lead to final systems design.

DIGITAL CORRELATOR STUDY

PART I

A. PURPOSE:

The study was to conduct a systems analysis and prepare a proposed design of a digital correlator for waveform classification purposes based on the following system parameters:

1. Maximum signal frequency of interest: 400 cps
2. Signal amplitude resolution: 32 levels
3. Range gate: target range ± 1000 yards
4. Pulse repetition intervals: 8-25 seconds
5. Pulse width: 10 milliseconds to 1 second

On-line classification was to be given priority over off-line procedures, and various designs were to be investigated with comparisons made for each system.

B. GENERAL FACTUAL DATA:

Personnel: The following personnel were employed in this study for the periods indicated.

R. B. Arndt, Principal Systems Design Engineer:	1.5 man months
G. F. Marette, Principal Systems Design Engineer:	4.0 man months
E. J. Farrell, Mathematician:	4.7 man months
R. R. Lachenmayer, Associate Systems Design Eng:	5.8 man months

C. DETAILED FACTUAL DATA:

1. Algorithm Determination. The initial approach to the correlation problem was based on the generation of a sum-of-products correlation between the range-gated unknown waveform and a library of standard waveforms. The correlator design was to be based on the availability of an AN/USQ-20 Unit Computer during the time required for the classification procedure.

Several methods were considered for implementing the sum-of-products computation, but because of the stringent time requirements of the on-line problem these methods were narrowed down to two: residue arithmetic and carry-store addition. The residue arithmetic was attractive because of the fast multiply and add times available in this system. These fast times result because there is no propagation of carries or borrows between residue groups. Disadvantages of the residue system are the conversions required between residue and binary representation at the input and output, and there is no practical method for comparing two residue numbers. This was particularly important since classification would be determined by the maximum correlation values computed.

The second method, the carry-store addition, was selected for use because it did not have the conversion and comparison limitations of the residue system, and could be operated at fast speeds for the size of the numbers involved. In this method the products are accumulated by a series of half adds, where the carries are stored, and are not allowed to propagate more than

one stage for each half add. At the end of the last product addition, the carries are allowed to propagate through the carry pyramid to obtain the final sum-of-products. The amount of extra time required for the final propagation of carries is not significant and therefore the total multiply-add time is essentially the time required to do the half adds.

In most digital multipliers, the multiplier is examined one bit at a time and the multiplicand or zero is added to the accumulated product, if the multiplier bit being sampled is a binary "1" or "0", respectively. The multiplicand must be scaled by powers of two depending upon the location of the "1" within the multiplier word. If this method were used, it would take five half add times to complete each sample by sample multiplication. This time would be excessive for the problem under study, so it was decided to examine the multiplier in two increments instead of five. The first sampling of the multiplier examines the lower 3 bits and the second sampling examines the upper two bits and the carries from low order bits. Monthly Status Report #3 presents a detailed description and example of this multiplication procedure. The end result of this scheme is that it allows the multiplications for 5-bit samples to be completed in two half add times instead of five.

2. Timing Considerations. With the multiplication scheme selected, the system parameters affecting speed were examined to determine a practical clock rate. The factors affecting this were: the maximum pulse repetition rate of 8 sec., the length

of the standard reference waveforms, the sampling frequency, and the number of stored reference waveforms. The first calculation assumed the number of stored reference waveforms to be 1000. The number of 5-bit multiplies and the time per multiply were plotted as a function of sampling frequency and standard waveform size. These results are shown in Figures 1 and 2, respectively. From Figure 1 it can be seen that for a sampling frequency of 800 cps. and a standard waveform length of 150 yards, there would be 277×10^6 5-bit multiplications in 8 seconds. Figure 2 shows that this would allow a maximum of 30 nanoseconds per multiply or 15 nanoseconds per half add which is impractical in terms of the present state of the computer art.

In view of the above, it was decided to utilize circuitry, developed for Project Lightning, operating with a four-phase, 4-megacycle clock that results in a 16-megacycle transfer rate. With the clock rate thus fixed, another series of calculations were run to determine the number of standard waveforms that could be referenced as a function of sampling frequency and standard waveform size. The results of these calculations are shown in Figure 3. From this graph one can see the various trade-offs possible at different sampling rates for the standard waveform sizes shown. For example, for a sampling frequency of 800 cps and standard waveform size of 150 yards, there is time to perform a sum-of-products correlation with 115 standard waveforms in 8 seconds. At a sampling frequency of 400 cps and the same

Figure 1

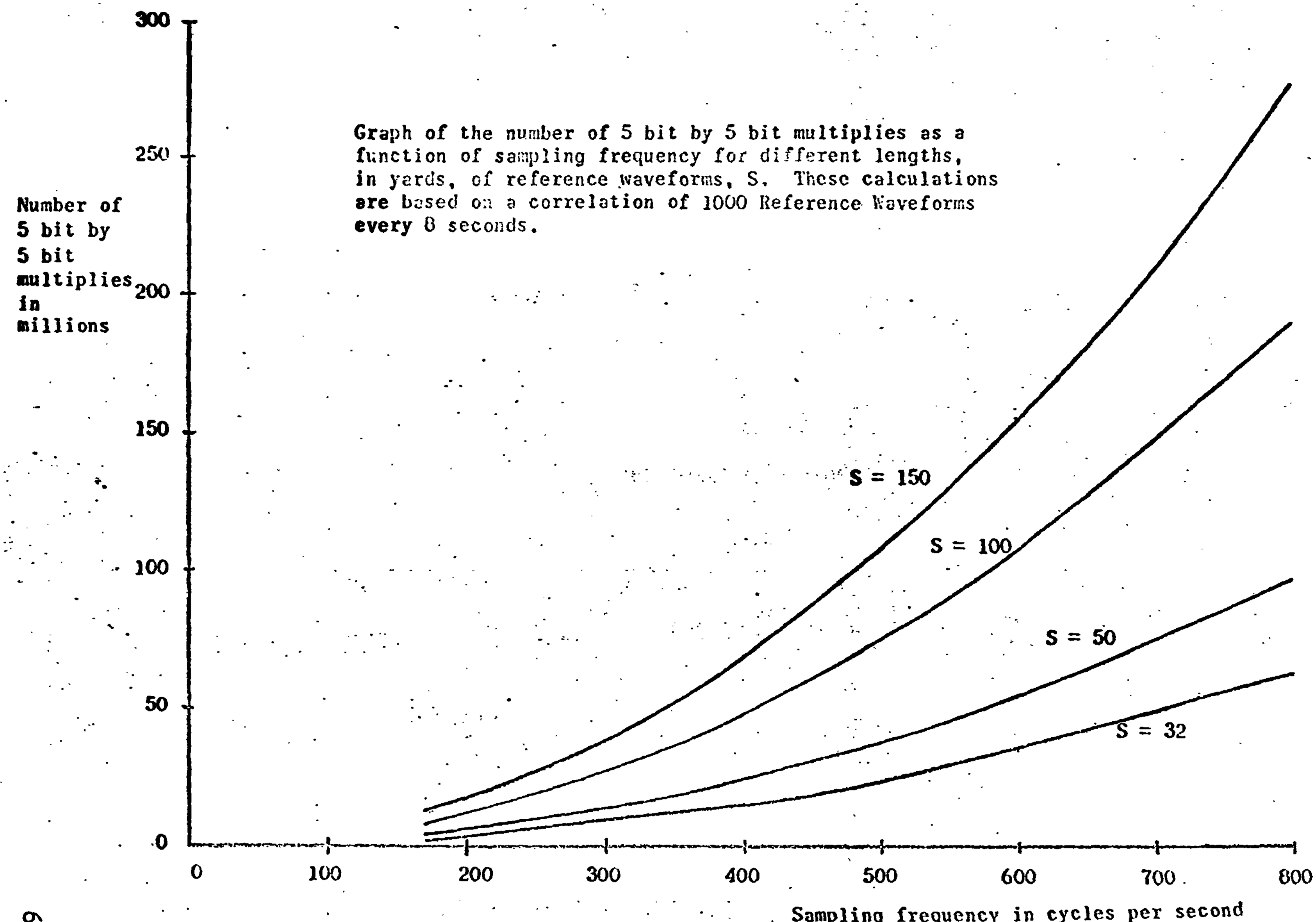

Graph of the number of 5 bit by 5 bit multiplies as a function of sampling frequency for different lengths, in yards, of reference waveforms, S. These calculations are based on a correlation of 1000 Reference Waveforms every 8 seconds.

Figure 2

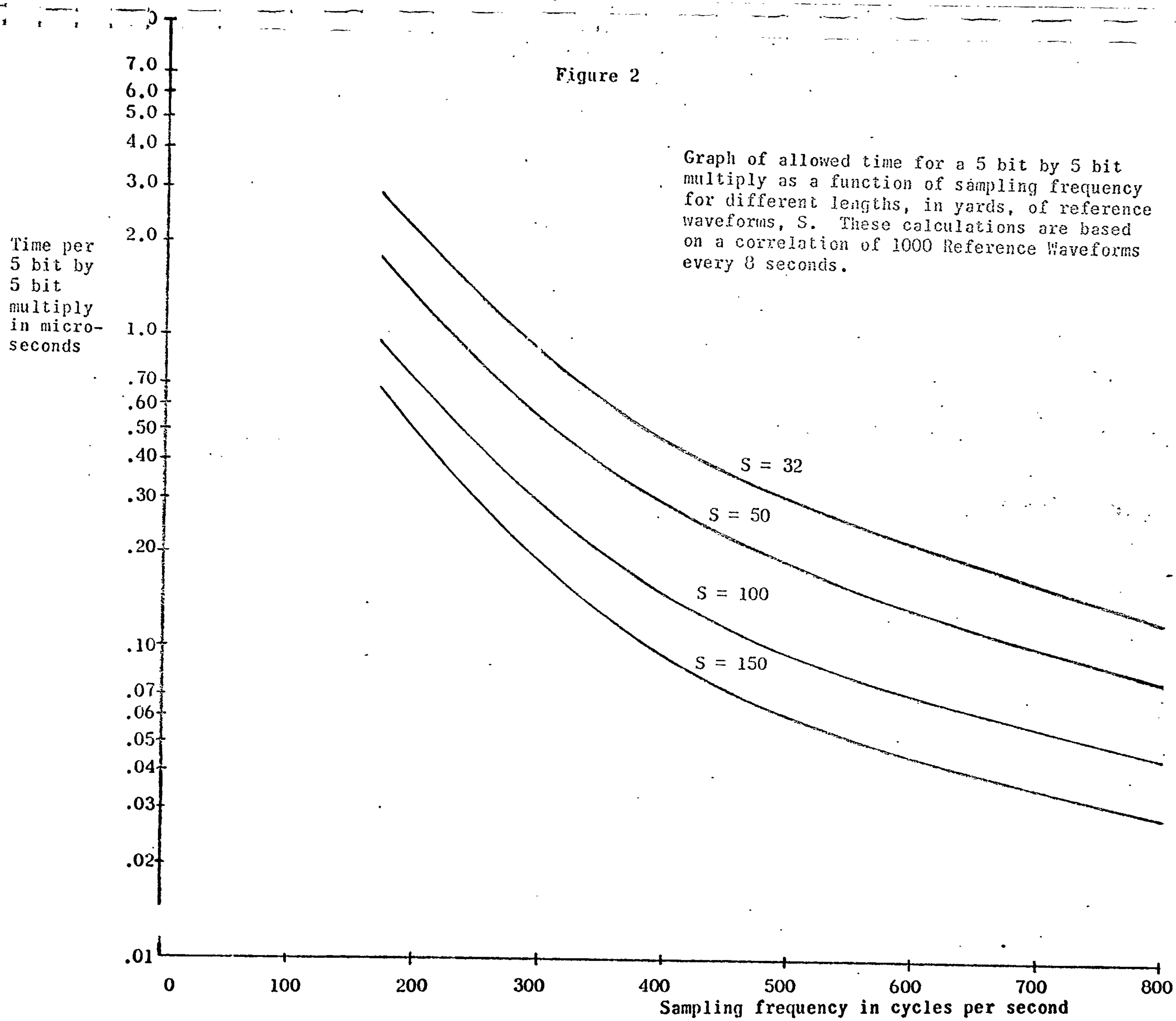

Graph of allowed time for a 5 bit by 5 bit multiply as a function of sampling frequency for different lengths, in yards, of reference waveforms, S. These calculations are based on a correlation of 1000 Reference Waveforms every 8 seconds.

Figure 3

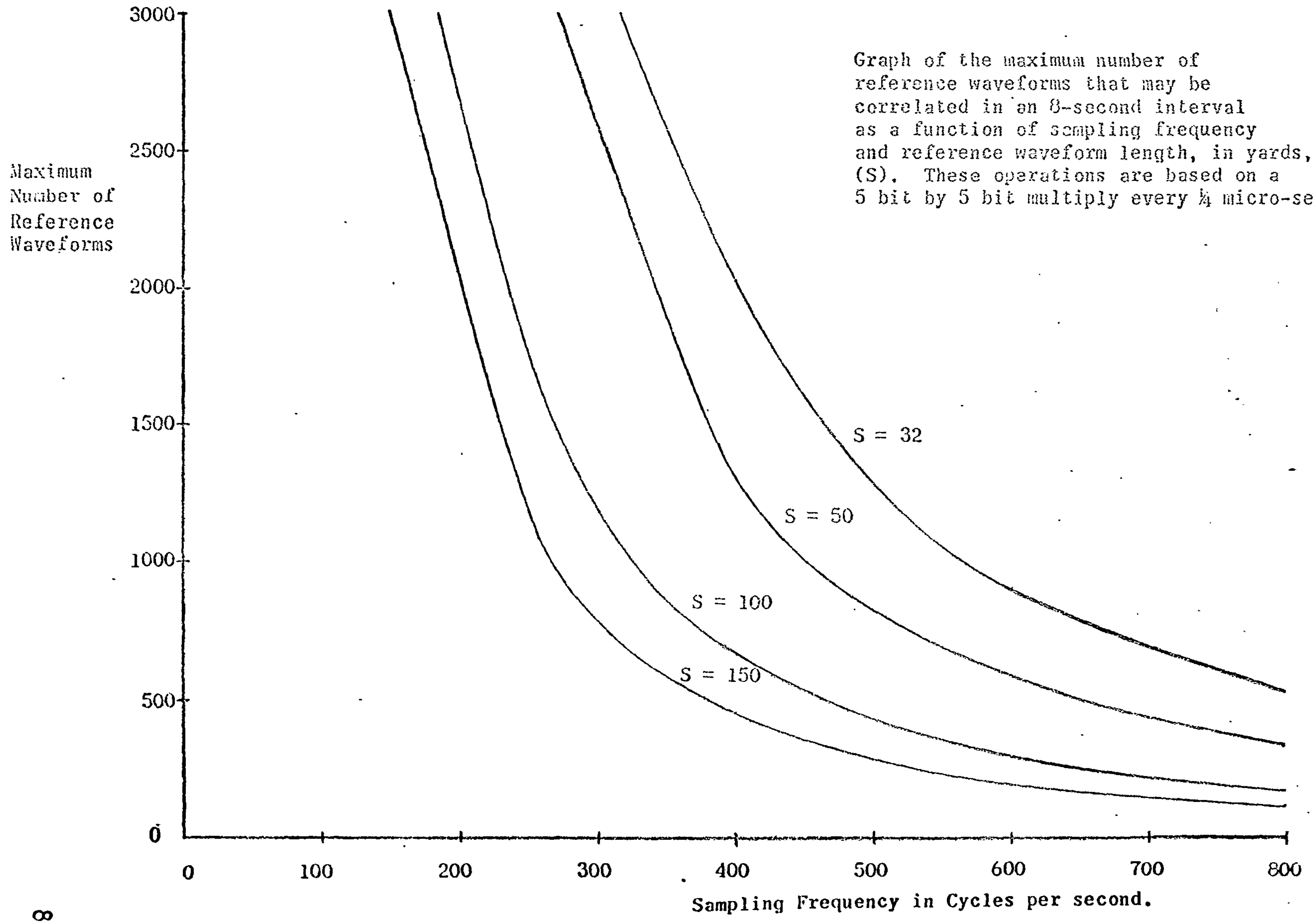

Graph of the maximum number of reference waveforms that may be correlated in an 8-second interval as a function of sampling frequency and reference waveform length, in yards, (S). These operations are based on a 5 bit by 5 bit multiply every ¼ micro-second.

standard waveform size, the number of waveforms increases to 462. Also, as the size of the standard waveform is reduced, the number of standard waveforms increases.

3. Sum of Products System.

(a) System Description

Since these results indicated that the assumed clock rate could be used to correlate over a large number of standard waveforms for different trade-offs of sampling frequency and standard waveform lengths, a feasibility design utilizing the AN/USQ-20 Unit Computer was completed to determine the approximate number of circuits that would be required to implement a correlator. This design used the sum-of-products method of which a block diagram is shown in Figure 4.

In reference to Figure 4, the standard waveform is stored during correlation in registers R_0 thru R_5. Registers R_6 and R_7 are used to shift the standard waveform by the sample size in a circular manner in conjunction with the other R registers. The quantized range gate samples are held in registers G_0 thru G_5. Registers G_6 and G_7 are used to shift the range gate information in much the same manner as registers R_6 and R_7 shift the standard waveform samples. Since the range gate information is correlated at one-sample offsets, another holding register G_{in}, is provided to supply the additional sample required for each offset.

Figure 4

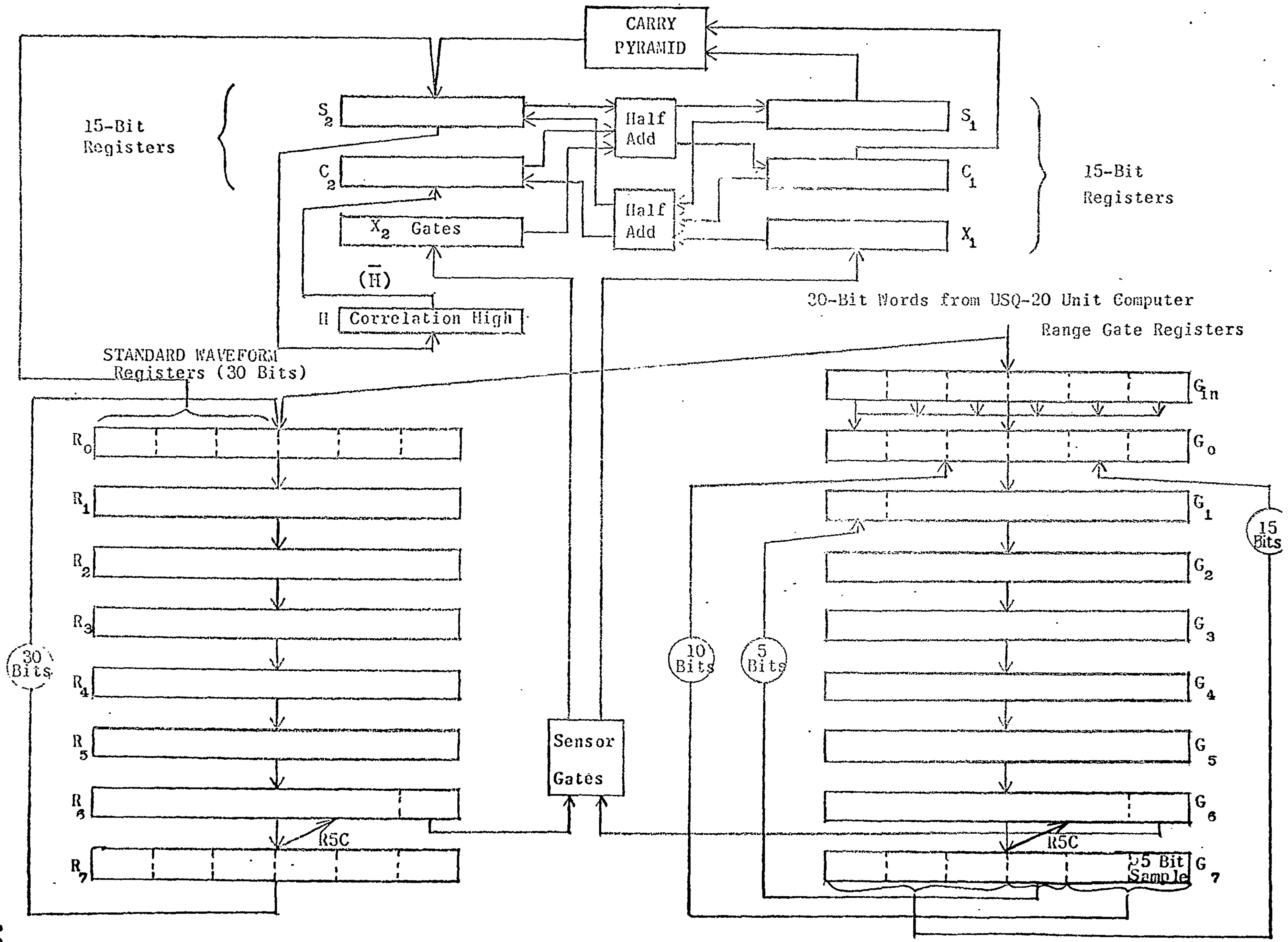
CARRY PYRAMID
15-Bit Registers
S_2
C_2
X_2 Gates
$(\bar{H})$
H Correlation High
Half Add
Half Add
S_1
C_1
X_1
15-Bit Registers
30-Bit Words from USQ-20 Unit Computer
Range Gate Registers
STANDARD WAVEFORM Registers (30 Bits)
R_0
R_1
R_2
R_3
R_4
R_5
R_6
R_7
R5C
30 Bits
Sensor Gates
G_{in}
G_0
G_1
G_2
G_3
G_4
G_5
G_6
G_7
15 Bits
10 Bits
5 Bits
R5C
5 Bit Sample

The lower five bits of register G_6 act as the multiplier for each operation, and the corresponding bits of R_6 are the multiplicand. The multiplier is examined in two increments; the lower three bits first and then the upper two bits. This is accomplished by the sensors shown in the block diagram of Figure 4 as the sensor gates. The result of the first sensing operation will be to gate the appropriate multiple of the multiplicand through the X_2 gates to be half added with the quantities in the S_2 and C_2 registers. The second sensor will control the transmission of another multiple of the multiplicand to the X_1 register where it will be half added with the quantities in the S_1 and C_1 registers. The S_1, C_1 and S_2, C_2 registers contain the stored bit sums and carries resulting from the half adds.

In practice each standard waveform would contain a constant which would be a combination of normalizing, probability, and threshold constants. This constant would be initially entered into the S_2 register by the transmission path shown from the R_0 register to the S_2 register in Figure 4. At the completion of the multiply-add operation for each offset of the range gate information, the resulting sum is compared to the highest previous correlation value obtained for that specific standard waveform. If the resulting sum is greater, it is stored in the H register, which holds the high correlation value.

(b) Control

A flow chart illustrating the control sequence is shown in Figures 5 and 6. For the purpose of this illustration, it will

be assumed that all registers of Figure 4 will be in the cleared state, and that the range gate and 1000 standard waveforms are stored in the memory of the AN/USQ-20 Unit Computer. The loading sequence, Figure 5, is initiated by the sonar operator. On the "start" command the loading of the first standard waveform is begun. As the loading sequence of the first standard waveform is completed, the loading of the range gate waveform is initiated. At its completion, the actual correlation process is begun as shown in Figure 6 and repeated through the 1000 standard waveforms, at which time the correlation value will be displayed and the loading and correlation sequences terminated.

4. Statistical Analysis. While the sum-of-products design was being completed, analysis of the general problem of waveform classification was continuing. Reasonable criteria for selecting a classification procedure lead to procedures that have the same general form and differ only in the value of certain parameters. A detailed discussion and derivation is presented in the attached report. Basically the procedures "correlate" the input return with all of the standard returns, and select the standard return with the highest "correlation". The "correlation" value used to compare the standard returns is the usual product-sum correlation corrected by an additive constant. If $(u_{i1}, u_{i2}, \ldots, u_{in})$ represents the i-th standard return, and $(x_1, x_2, \ldots, x_n)$ represents the input return, the optimum procedure compares

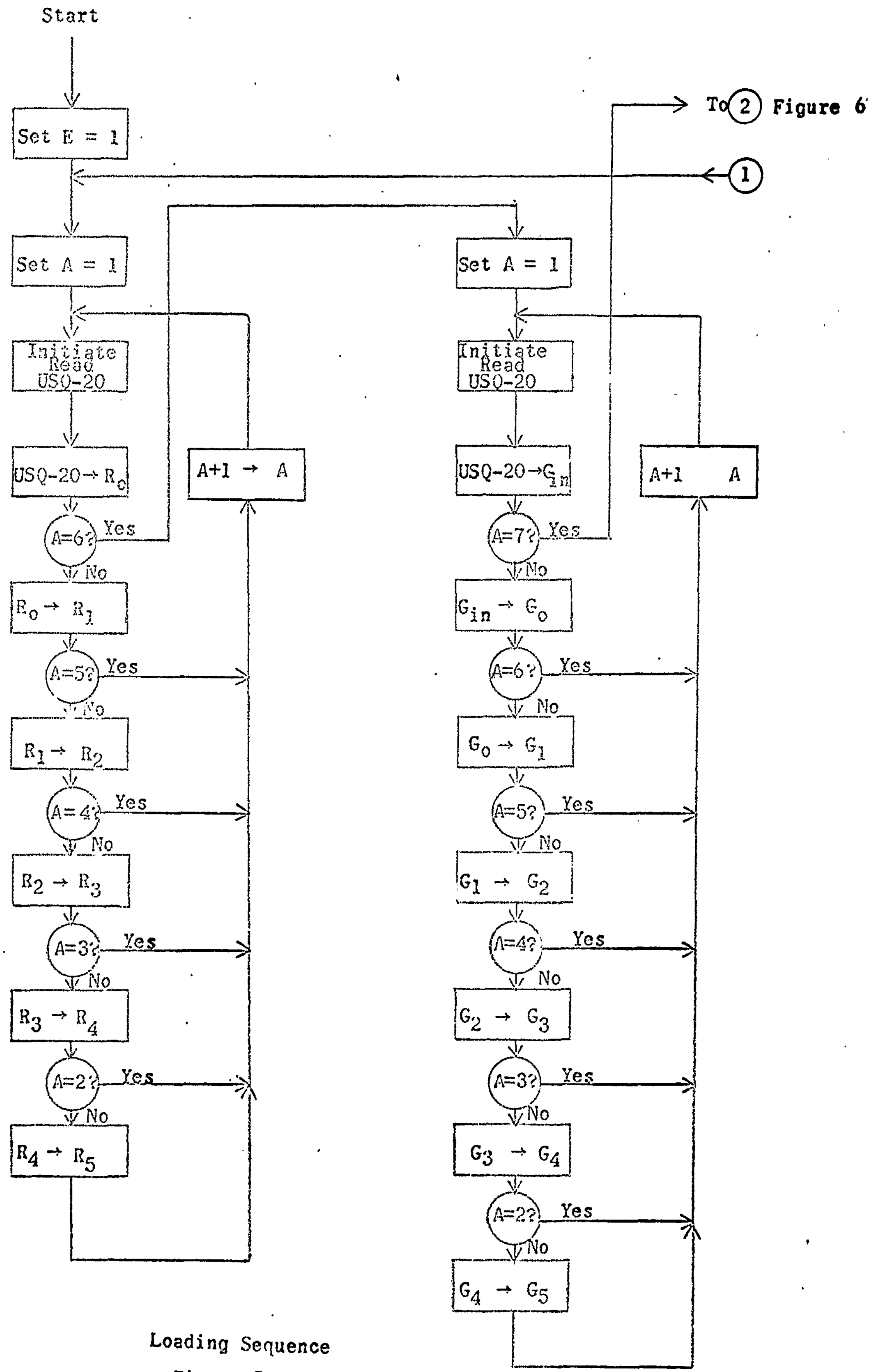

Loading Sequence

Figure 5

Correlation Sequence

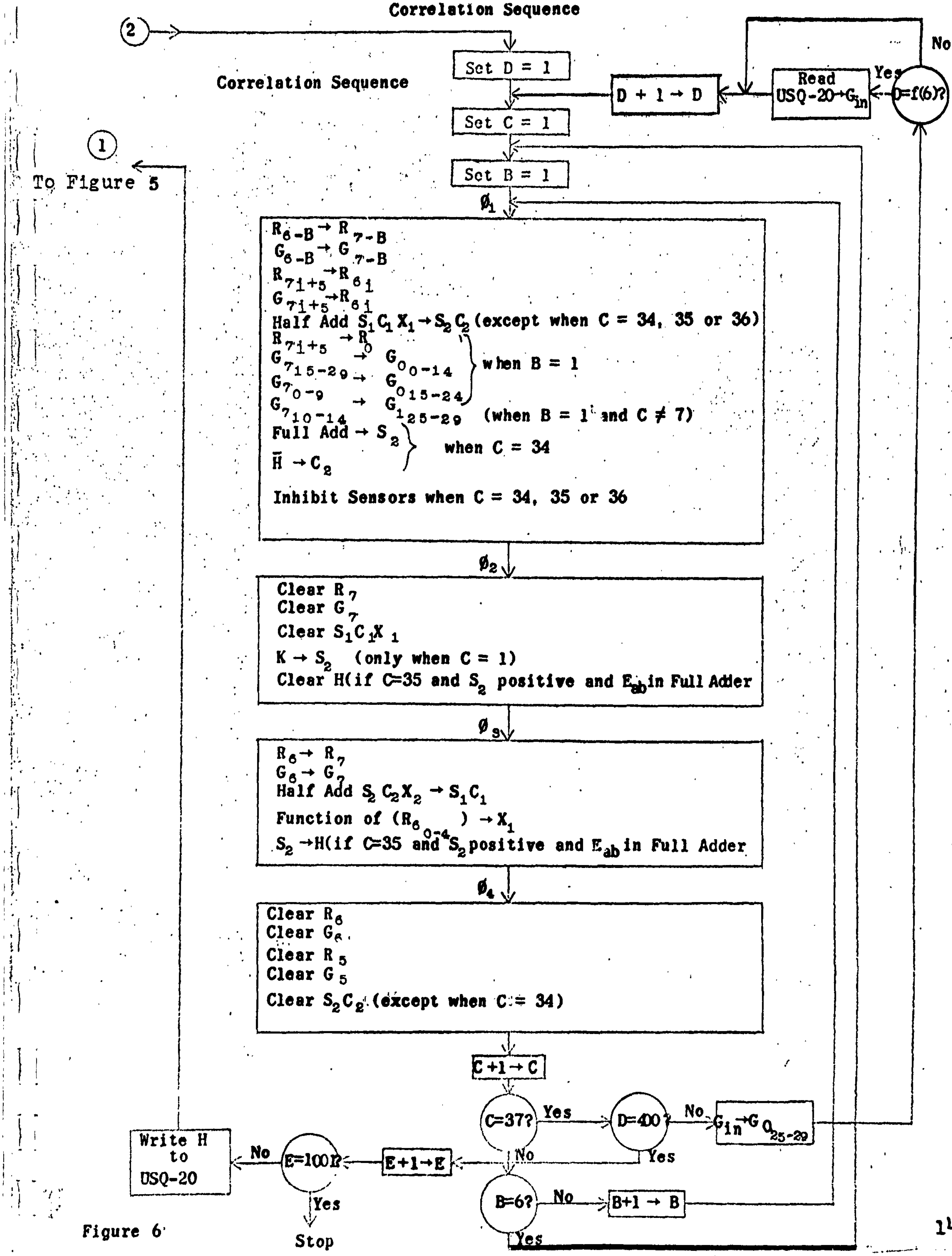

Figure 6

$$2(\overline{\eta^2} - \overline{\eta}^2)\log(w_1\lambda_1) - \sum_{r=1}^{n}(u_{1r}+\overline{\eta})^2 + 2\sum_{r=1}^{n}(u_{1r}+\overline{\eta})x_r ,$$

$$2(\overline{\eta^2} - \overline{\eta}^2)\log(w_2\lambda_2) - \sum_{r=1}^{n}(u_{2r}+\overline{\eta})^2 + 2\sum_{r=1}^{n}(u_{2r}+\overline{\eta})x_r ,$$

$$2(\overline{\eta^2} - \overline{\eta}^2)\log(w_3\lambda_3) - \sum_{r=1}^{n}(u_{3r}+\overline{\eta})^2 + 2\sum_{r=1}^{n}(u_{3r}+\overline{\eta})x_r ,$$

etc., where $\overline{\eta}$ is the average (or d.c.) noise level and $\overline{\eta^2}$ is the average squared noise level (or average noise power). The value of the parameters λ_i and w_i depend on criterion used in selecting a classification procedure.

For example, if the goal is to maximize the average probability of correct classification, $w_i = 1$ for all values of i and λ_i is the relative frequency (or a priori probability) that the input return is from the i-th target. Introducing a priori probabilities has the effect of favorably weighting those standard returns that occur more often. The influence of this weighting increases with the noise power; if the noise level is high, the classification procedure relies more on a priori probabilities than on the input return. If the a priori probabilities change from one region of the ocean to another, one can adjust the classification procedure by changing the λ_i's. Similarly, if

the noise power increases due to changes in target range or position of the sonar, one can adjust the classification procedure by changing $\overline{\eta^2}$. Note that $u_{ir} + \bar{\eta}$ is obtained by averaging several returns from a known target.

Several assumptions were made to arrive at the above classification procedure: viz.,

i) The range of the target is known.

ii) The input to the digital correlator has been corrected for range attenuation; the input return and standard returns have comparable amplitudes. The "signal to noise" ratio may change with range.

iii) The quantized (in amplitude) samples from the input return can be approximated by continuous samples.

iv) The noise is a superposition of randomly positioned pulses with random amplitudes; i.e., the noise is Gaussian.

v) The noise characteristics are constant over the range gate: constant average, constant power, etc.

vi) The noise spectrum has a sharp high frequency cutoff; and the sampling frequency is twice this cutoff frequency.

In practice, the exact range of the target is unknown and the range gate must be searched. In this case, another term must be added to the correlation value: viz., $-\sum_{r=1}^{n} x_r^2$. In our

analysis of classification with a known range, this term appears as a "constant" in comparing the standard returns and was dropped. Introducing this term, the classification procedure becomes a comparison of

$$2(\overline{\eta^2} - \overline{\eta}^2)\log(w_1\lambda_1) - \sum_{r=1}^{n}(u_{1r} + \overline{\eta} - x_r)^2 ,$$

$$2(\overline{\eta^2} - \overline{\eta}^2)\log(w_2\lambda_2) - \sum_{r=1}^{n}(u_{2r} + \overline{\eta} - x_r)^2 ,$$

$$2(\overline{\eta^2} - \overline{\eta}^2)\log(w_3\lambda_3) - \sum_{r=1}^{n}(u_{3r} + \overline{\eta} - x_r)^2 , \quad \text{etc.}$$

Basically, this classification procedure is a comparison of the least squared deviation between the input return and the various standard returns.

5. Least Squared Difference Method. Since the least squared difference method appeared attractive, a design utilizing this method was completed. The desired result of the least squared difference method is

$$\sum_{r=1}^{n} (R_r - G_r)^2 = \text{correlation value}$$

where R represents the quantized amplitude of the stored reference

waveforms and G represents the quantized amplitude of the raw video waveform.

Figure 7 is a block diagram of the correlator implementing the above process. Comparing Figure 7 with Figure 4 shows the elimination of the 30-bit registers R_7 and G_7 plus associated circuitry.

The remaining R and G registers continue to perform the function of holding the standard waveform and a portion of the range gate return during the correlation process. The shifting formerly done between registers G_6 and G_7 and between R_6 and R_7 has been eliminated. The same effect is now obtained by gating directly out of the appropriate sections of G_6 and R_6. The two blocks labeled $(R-G)^2$ subtract one five-bit sample in G from one five-bit sample in R, square the difference, and then transfer it to their respective X_1 or X_2 registers. The S and C registers and the half adders continue to perform the summation process. The H register is used to store the current correlation sum for comparison with the latest result.

This design along with the sum-of-products design had the disadvantage of being limited by the input/output speed of the AN/USQ-20 Unit Computer. The least-squared-difference system was capable of operating at twice the speed of the sum-of-products system, but since both systems were limited by the speed of the AN/USQ-20 Unit Computer, the main advantage of the least-squared-difference method was that slower, less expensive circuits could

Figure 7

Block Diagram of Correlator Utilizing $\sum (R-G)^2$ Process

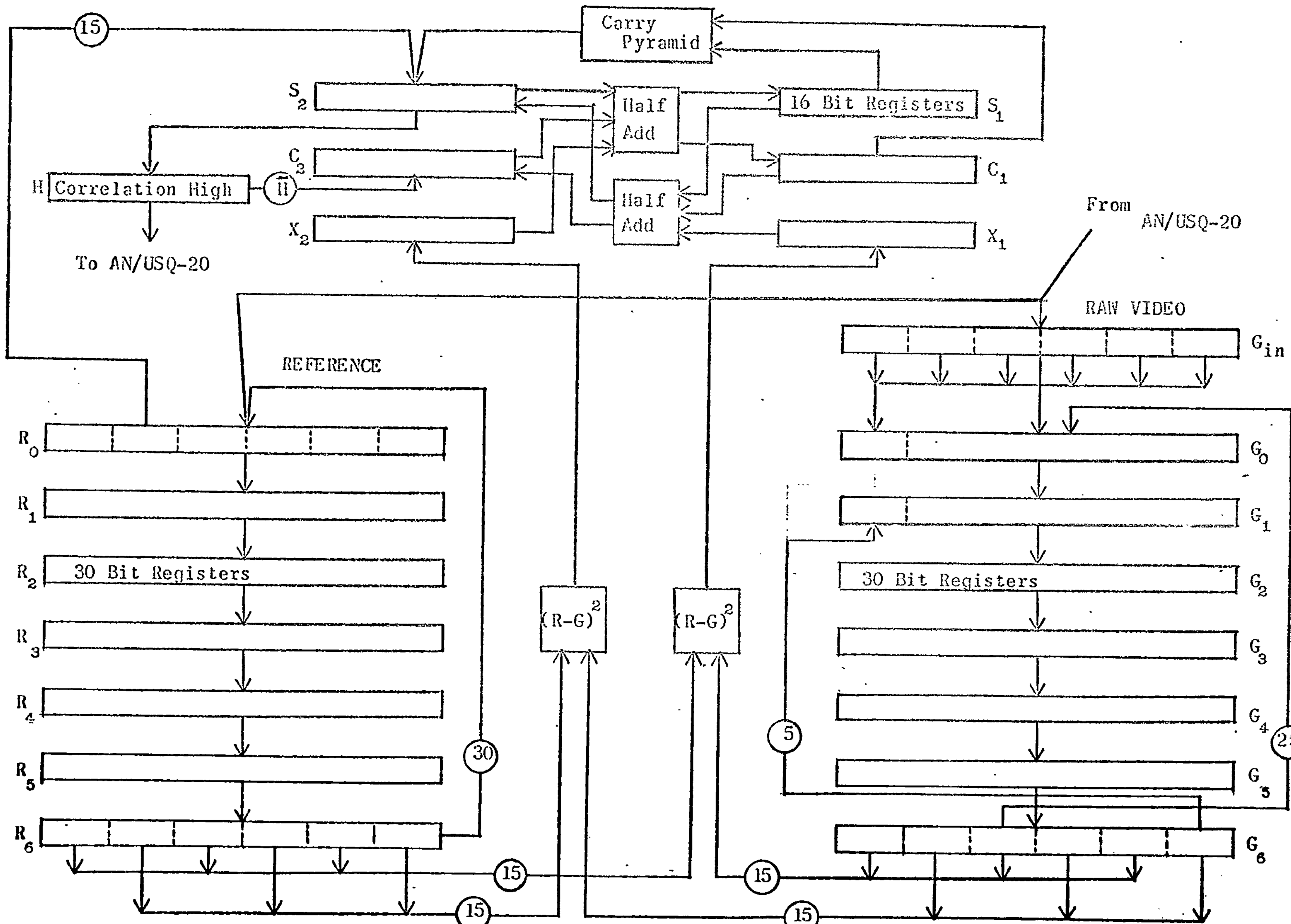

be utilized in the design. Another disadvantage of both of the aforementioned designs, was the need for holding registers for both the standard waveform and a portion of the range gate waveform. These registers would have to be equal in length to the size of a standard waveform. For large standard waveforms, high sampling rates, and greater number of levels of quantitization, the number of circuits required for these holding registers becomes many times greater than the number of circuits required for the arithmetic operations. This can be seen in Table I which is a tabulation of the approximate number of inverters required to implement either of the two systems for various sampling frequencies and standard waveform sizes. The numbers in the columns labeled R & G represent the inverters required for the two holding registers. The last column shows the percentage of the total number of inverters required for the holding registers.

6. <u>Separate Memory Systems</u>. In order to take advantage of the speed of the least-squared-difference method and to partly eliminate the need for the many holding registers, a system design utilizing a separate memory for the quantized range gate waveform was investigated. A block diagram of this system is shown in Figure 8. Besides operating at twice the speed of the previous least-squared-difference system, this design has eliminated most of the holding registers required for the range gate waveform. Two registers, G_0 and G_1 , are required external to the memory for shifting purposes. These registers are one sample size greater

	Sampling Frequency	Yards per Sample	Number of Samples	Number of Inverters						$\frac{G + R}{Total} \times 100\%$
				Carry Pyramid	Half Add	S, C, X, H	G	R	Total	
S = 150 yards	170	4.7	32	144	288	450	870	780	2532	65
	250	3.2	47	153	306	468	1050	960	2937	68
	400	2	75	162	324	496	1500	1410	3892	75
	600	1.33	113	162	324	496	2040	1950	4972	80
	800	1	150	171	342	519	2580	2490	6102	83
S = 100 yards	170	4.7	22	144	288	450	690	600	2172	60
	250	3.2	32	144	288	450	870	780	2532	65
	400	2	50	153	306	468	1140	1050	3117	70
	600	1.33	75	162	324	496	1500	1410	3892	75
	800	1	100	162	324	496	1830	1740	4552	79
S = 50 yards	170	4.7	11	135	270	397	510	420	1732	54
	250	3.2	16	135	270	397	600	510	1912	58
	400	2	25	144	288	450	690	600	2172	60
	600	1.33	38	153	306	468	960	870	2757	66
	800	1	50	153	306	468	1500	1410	3892	75
S = 32 yards	170	4.7	7	117	234	355	410	330	1446	51
	250	3.2	10	135	270	397	510	420	1732	54
	400	2	16	135	270	397	600	510	1912	58
	600	1.33	25	144	288	450	690	600	2172	60
	800	1	32	144	288	450	870	780	2532	65

TABLE 1

Block Diagram of Correlator Employing A Range Gate Memory

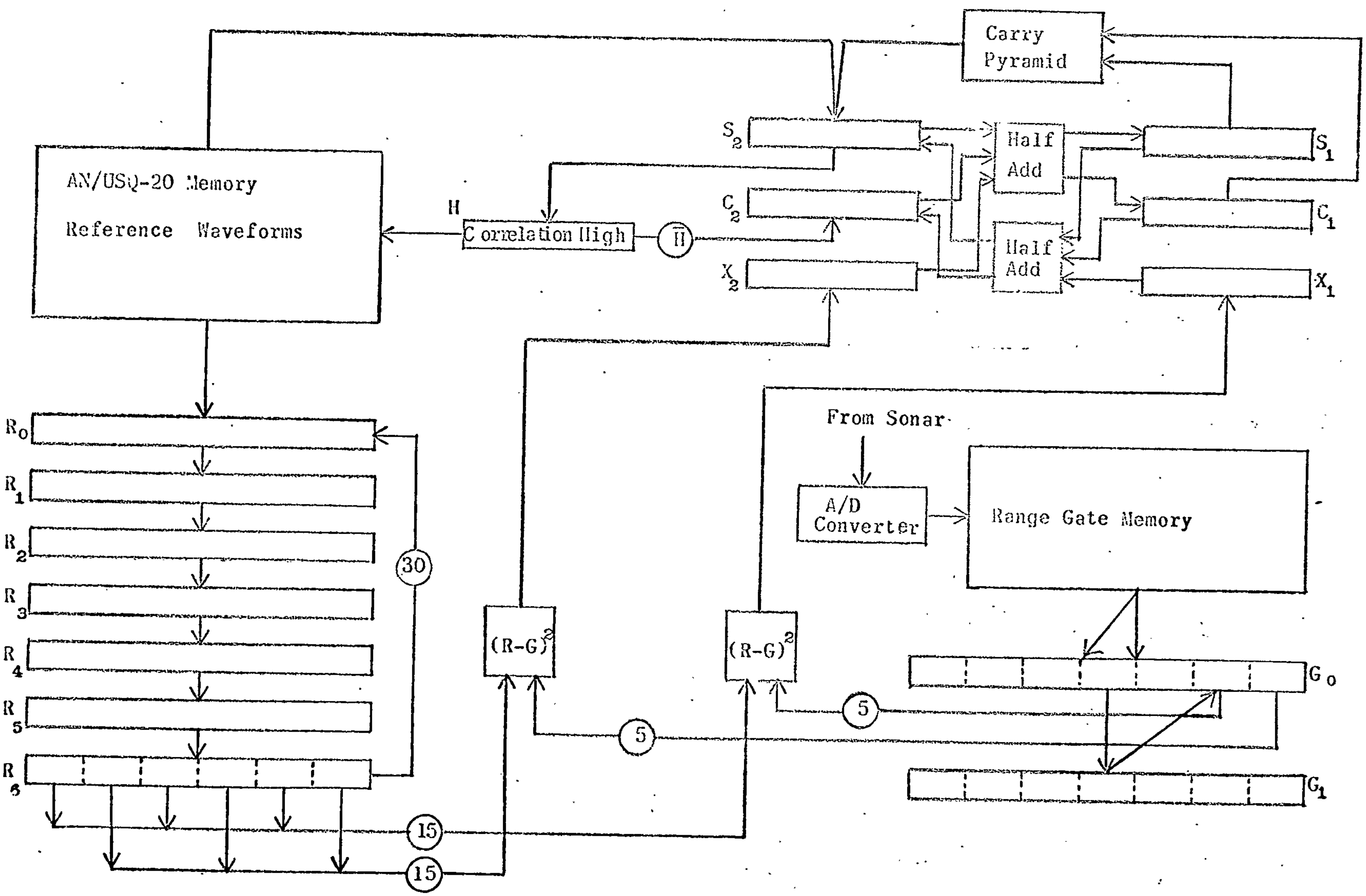

Figure 8

than the word length of the memory. This was necessitated to allow for one sample offsets in the correlation process across the range gate samples.

In the initial phases of the study, it was assumed that the AN/USQ-20 Unit Computer would be available for use in the target classification process, and that memory space and input/output channels would also be available for these purposes. Later discussions with Bureau of Ships personnel have cast some doubt upon the validity of these assumptions. Because of this and the fact that the holding registers required for the standard reference waveforms can be very large at high sampling frequencies, another system was studied which included a separate memory for the reference waveforms. A block diagram of this system is shown in Figure 9.

This system is completely independent of the AN/USQ-20 Unit Computer. The high values of correlation are stored in the reference waveform memory and the control portion of the correlator updates these values after each reference waveform is completed. A disadvantage of this system is that extra circuitry must be added to enter reference waveform information from a peripheral storage device such as a magnetic tape unit. The reference waveform memory would also have to be faster than the AN/USQ-20 Unit Computer memory since it would have to keep pace with the speed of the correlation process. With a transfer rate of 16 megacycles, two samples from each waveform would be subtracted, squared, and summed

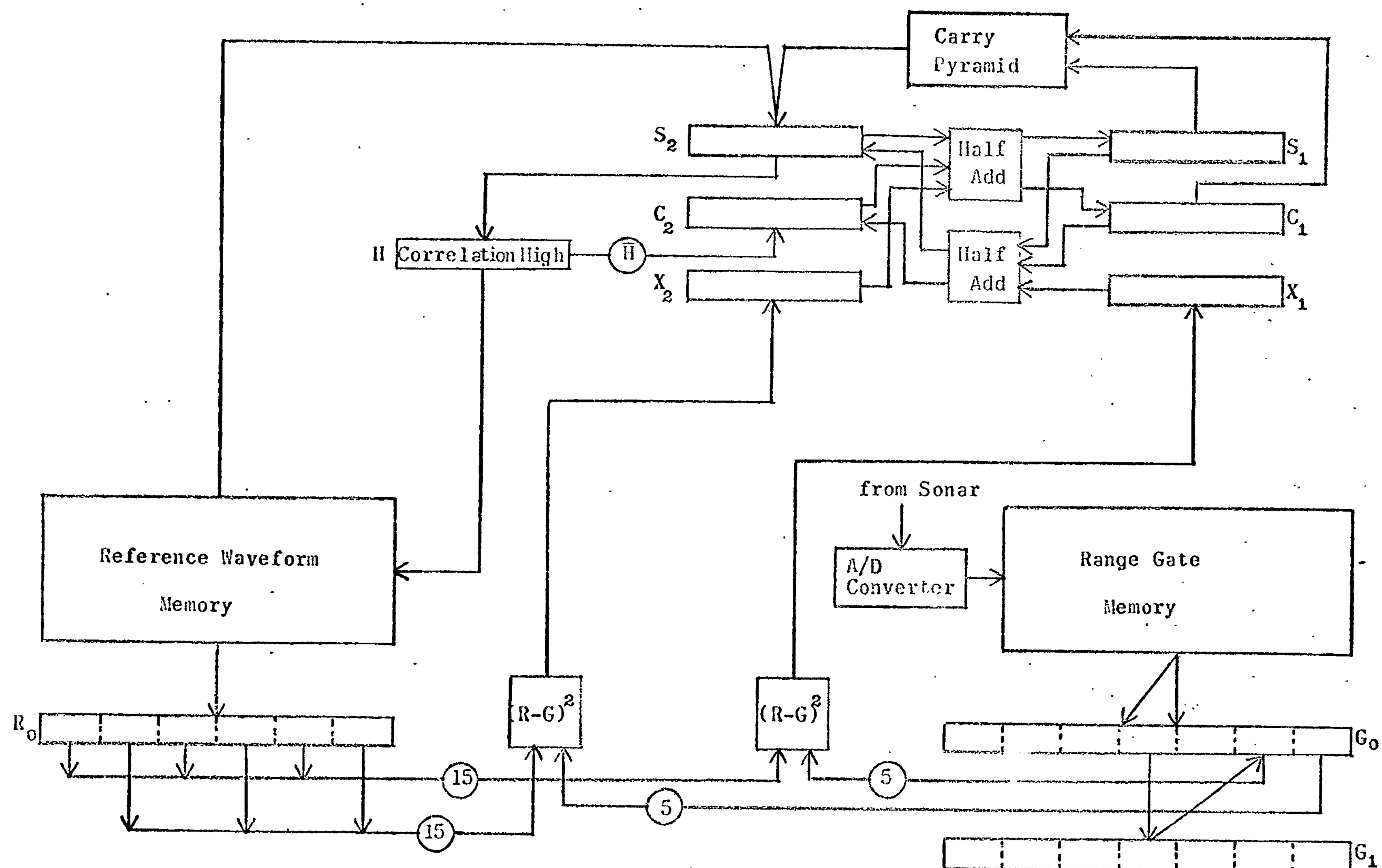

Block Diagram of Correlator Employing
Range Gate and Reference Waveform Memories.

Figure 9

every 1/4 μsec. Therefore a memory word length of 6 samples requires a new word to be read every 3/4 μsec. If a larger word length were selected, the memory cycle time would be increased proportionally.

7. Sonar Recording Observations. A group of sonar returns were made available by the Underwater Sound Laboratories in the last phases of this study. Some of these returns were recorded for a cursory visual inspection. Figure 10 shows a submarine return at four different speeds plus a representative whale return. The filtering evidenced in Figures 10a, b, c and e is a result of mechanical filtering introduced by the strip recorder. Figure 10d shows the 800-cycle component from the AN/SQS-23 audio channel.

The initial examinations seem to indicate that each target has a representative waveform or class of waveforms that are not similar to the whale returns. Since none of the targets on the tapes were identified according to nature, size, or aspect, the results could not be extended to include any detailed analysis of the observed waveforms.

D. CONCLUSIONS:

The resulting designs and study have shown that a digital correlator for the classification of sonar waveforms is practical from both the mathematical and hardware viewpoints. For a sampling frequency of 800 cps, a standard waveform size of 150 samples, and the maximum pulse repetition rate of 8 seconds, it is possible to correlate over 200 reference waveforms. As these

Recorded Sonar Returns

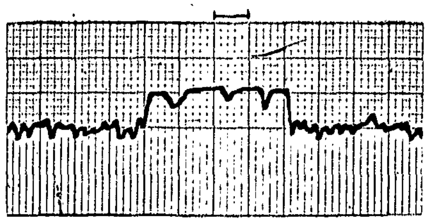

(a) Submarine

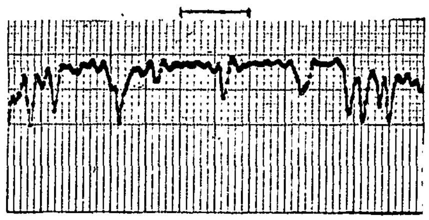

(b) Submarine

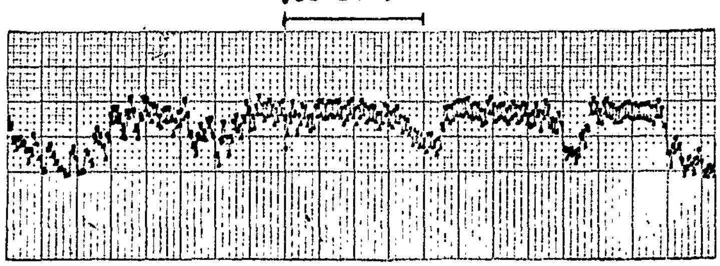

(c) Submarine

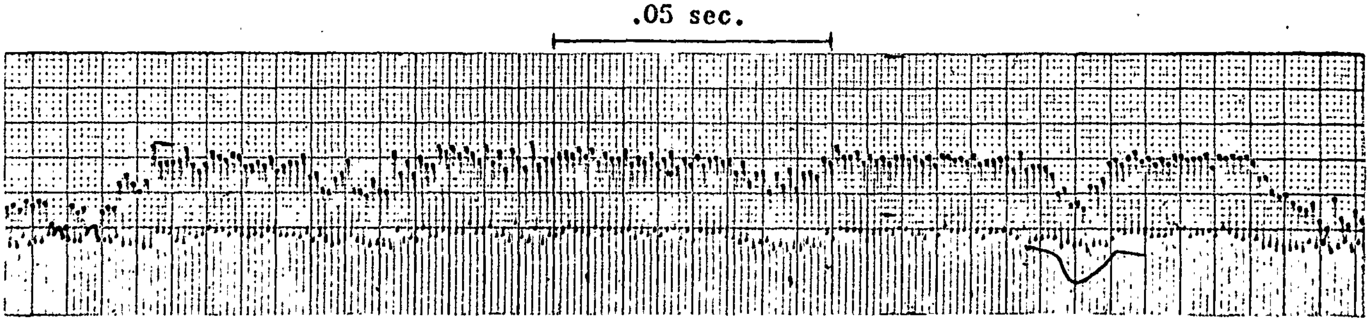

(d) Submarine

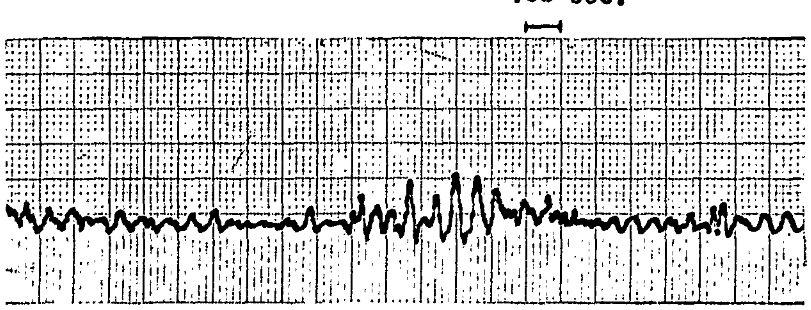

(e) whale

Figure 10

parameters are relaxed, it is possible to correlate greater numbers of reference waveforms. The procedures developed also allow for changes in noise level and for differences in the frequency of occurrence of various targets.

PART II

RECOMMENDATIONS

Since the method proposed is relatively unique for the classification of sonar returns, there are several unknowns that will affect the selection of a specific design. Some of these are:

1) number of different waveforms needed to represent a specific target (or class of targets) at various aspects.
2) sampling frequency which is sufficient to identify different types of targets
3) length of standard reference waveforms necessary to uniquely identify a target or class of targets
4) number of levels of quantitization necessary for accurate identification
5) number of sample offsets in the range gate waveform to effect a correct identification with the standard reference waveforms
6) the availability of the AN/USQ-20 Unit Computer for the correlation process.

It is recommended that the above areas be studied further to determine the optimum parameters for a specific design. A simulation phase has been proposed that will simulate the mathematical procedures recommended with actual sonar returns. The simulation, besides determining the validity of the methods recommended, will be used with variations in the system parameters to obtain a final recommended system design.

For the extended study and simulation the recordings of sonar returns must contain explicit information regarding the targets. This will be necessary for the formulation of the standard reference waveforms and also to determine the accuracy of the simulated correlation process.

Waveform Identification Using Digital Techniques

by

Edward J. Farrell

EF 2459-35

Mathematics & Logic Research Department

October 2, 1962

UNIVAC
Division of Sperry Rand Corporation
St. Paul 16, Minnesota

Waveform Identification Using Digital Techniques

I. Introduction

Many problems of waveform identification or recognition can be formulated in the following way. Several standard waveforms are specified. Given one of the standard waveforms that has been changed by "noise", the problem is to identify the standard waveform. In many situations waveform identification is difficult and accurate comparisons must be made. For this reason digital techniques are preferred over analog. The noisy waveform and standard waveforms are digitized; i.e., they are represented by uniformly space samples. The noisy waveform is identified using these digitized waveforms. In the following paragraphs an identification procedure is derived.

II. Selection of an Identification Procedure

By applying certain methods of decision theory, one can select an identification procedure without additional restrictions on the problem. There are several criterion for selecting an identification procedure. The following criterion will be discussed:

i) average probability of correct identification,

ii) probability of correct identification for "least favorable" standard waveforms,

iii) probabilities of correct identification which are in a specified ratio.

Assume there are N standard waveforms. Let $p_i(I)$ be the probability of correct identification when the noisy waveform is the i-th standard waveform and identification procedure I is used. The average probability of correct identification is

$\sum_{i=1}^{N} \lambda_i p_i(I)$, where λ_i represents the a priori probability that the noisy waveform is the i-th standard waveform. The probability of correct identification for "least favorable" standard waveforms is $\min\{p_1(I), p_2(I), \cdots, p_N(I)\}$. The third criterion is of a different nature. In certain situations it may be desirable to have the $p_i(I)$'s in a specified ratio; i.e., $w_1 p_1(I) = w_2 p_2(I) = \cdots = w_N p_N(I)$, where the w_i's are positive. The goal is to select an identification procedure I^* that satisfies the above ratio

condition and for which there is no "uniformly better" procedure; i.e., there is no procedure I' such that $p_i(I^*) \leq p_i(I')$ for all i and $p_j(I^*) < p_j(I')$ for some j.

These criteria lead to identification procedures that have the same form and differ only in the value of certain parameters. Let $x = (x_1, x_2, x_3, \cdots, x_n)$ represent n uniformly-spaced samples of the noisy waveform. Let $f_i(x)$ represent the multivariate density function of x given the noisy waveform is the i-th standard waveform. The optimum identification procedure for all three criteria is of the form

$$I_\lambda : \begin{cases} \text{if } x \text{ is received and} \\ w_i\lambda_i f_i(x) = \max\{ w_1\lambda_1 f_1(x), \cdots, w_N\lambda_N f_N(x) \}, \\ \text{then select the i-th standard waveform.} \end{cases}$$

If $w_i = 1$ for all i and λ_i is the a priori probability that the noisy waveform is the i-th standard waveform, identification procedure I_λ maximizes the average probability of correct identification. If $w_i = 1$ for all i and if the λ_i's are selected so that

$$p_1(I_\lambda) = p_2(I_\lambda) = \cdots = p_N(I_\lambda),$$

then I_λ maximizes the probability of correct identification for "least favorable" standard waveforms. For specified w_i's, if the λ_i's are selected so that

$$w_1 p_1(I_\lambda) = w_2 p_2(I_\lambda) = \cdots = w_N p_N(I_\lambda),$$

then I_λ satisfies the third criterion, provided the λ_i's are positive. These statements are proven in the following paragraph.

An identification procedure I can be characterized by a collection of N sets in Euclidian n-space; i.e., if x is in the first set, select the first standard waveform, if x is in the second set, select the second standard waveform, etc. Let $X_i(I, x)$ be a function of x which is one when x is in the i-th set and zero otherwise. Note that

$$\sum_{i=1}^{N} X_i(I,x) = 1$$

for all I and x. Also

$$p_i(I) = \int X_i(I,x)\, f_i(x)\, dx,$$

where the integration is over all values of x. Using $X_i(I,x)$, it is easy to show that I_λ maximizes

$$\sum_{i=1}^{n} \lambda_i w_i p_i(I) \;.$$

First

$$\sum_{i=1}^{n} \lambda_i w_i p_i(I) = \sum_{i=1}^{n} \lambda_i w_i \int X_i\,(I,x) f_i(x) dx$$

$$= \int \sum_{i=1}^{n} \lambda_i w_i\, X_i(I,x) f_i(x)\; dx \;.$$

From the definition of I_λ it follows that

$$\sum_{i=1}^{n} \lambda_i w_i \chi_i(I_\lambda, x) f_i(x) \geq \sum_{i=1}^{n} \lambda_i w_i \chi_i(I, x) f_i(x)$$

for each x, and hence

$$\sum_{i=1}^{n} \lambda_i w_i p_i(I_\lambda) \geq \sum_{i=1}^{n} \lambda_i w_i p_i(I) .$$

If the λ_i's are selected so that $w_1 p_1(I_\lambda) = w_2 p_2(I_\lambda) = \cdots =$ $w_N p_N(I_\lambda)$, then

$$\min \{ w_1 p_1(I_\lambda), w_2 p_2(I_\lambda), \cdots \} = w_1 p_1(I_\lambda) =$$

$$\sum_{i=1}^{n} \lambda_i w_i p_i(I_\lambda) \geq \sum_{i=1}^{n} \lambda_i w_i p_i(I) \geq \min \{ w_1 p_1(I), w_2 p_2(I), \cdots \} .$$

If the λ_i's are positive, there is no uniformly better procedure. Assume there is a I' such that

$$p_i(I_\lambda) \leq p_i(I') \quad \text{all } i$$

and

$$p_j(I_\lambda) < p_j(I') \text{ for some } j.$$

Then $\sum w_i \lambda_i p_i(I_\lambda) < \sum w_i \lambda_i p_i(I')$, provided the λ_i's are positive; but this is a countradiction. It follows that I_λ is optimum for all three criteria; the proof is completed. In the folloing section, it will be shown that I_λ is relatively simple with Gaussian noise.

III. Identification with Gaussian Noise

Assume the density function $f_j(x)$ is from the exponential family; i.e., $f_j(x)$ can be expressed as

$$f_j(x) = a_j\ h(x)\ \exp\left(\sum_{r=1}^{n} b_{jr}x_r\right),$$

where $h(x)$ is independent of j, and where a_j and b_{jr} are independent of x. Note that

$$a_j = \left[\int h(x)\ \exp\left(\sum_{r=1}^{n} b_{jr}x_r\right) dx\right]^{-1}$$

since the integral of $f_j(x)$ is one. The identification procedure I_λ is a comparison of $w_1\lambda_1f_1(x)$, $w_2\lambda_2f_2(x)$, $w_3\lambda_3f_3(x), \cdots, w_N\lambda_Nf_N(x)$ for a given x. Since $h(x)$ appears as a constant factor in each expression, I_λ reduces to a comparison of $w_1\lambda_1a_1\ \exp\left(\sum_{r=1}^{n} b_{1r}x_r\right)$, $w_2\lambda_2a_2\ \exp\left(\sum_{r=1}^{n} b_{2r}x_r\right)$, etc., or equivalently a comparison of

$c_1 + \sum_{r=1}^{n} b_{1r}x_r$, $c_2 + \sum_{r=1}^{n} b_{2r}x_r$, etc., where $c_i = \log w_i\lambda_ia_i$.

If the noise is a superposition of randomally positioned pulses with random amplitudes, it can be approximated by Gaussian noise; $f_j(x)$ will be a multivariate normal density

$$f_j(x) = \left[\frac{\det(m_{rs})}{(2\pi)^n}\right]^{1/2} \exp\left[-\frac{1}{2}\sum_{r=1}^{n}\sum_{s=1}^{n}(x_r-u_{jr}-\eta)m_{rs}(x_s-u_{js}-\eta)\right]$$

where (m_{rs}) is the inverse of the covariance matrix of the noise, where $\bar{\eta}$ is the average (or d.c.) noise level, and where $(u_{j1}, u_{j2}, \cdots, u_{jn})$ represents the j-th standard waveform. The average noise level is assumed to be constant over the sampling interval. A Gauissian approximation is reasonable when the average density of the noise pulses is "high" and the variance of the amplitudes is "small". The normal density function is in the exponential family; the constants a_j and b_{jr} are

$$a_j = \exp\left[-\frac{1}{2}\sum_{r=1}^{n}\sum_{s=1}^{n}(u_{jr}+\bar{\eta})m_{rs}(u_{js}+\bar{\eta})\right]$$

$$b_{jr} = \sum_{s=1}^{n}(u_{js}+\bar{\eta})m_{sr}.$$

The procedure I_λ reduces to a comparison of

$$\log(w_1\lambda_1) - \frac{1}{2}\sum_{r=1}^{n}\sum_{s=1}^{n}(u_{1r}+\bar{\eta})m_{rs}(u_{1s}+\bar{\eta}) + \sum_{r=1}^{n} b_{1r}x_r,$$

$$\log(w_2\lambda_2) - \frac{1}{2}\sum_{r=1}^{n}\sum_{s=1}^{n}(u_{2r}+\bar{\eta})m_{rs}(u_{2s}+\bar{\eta}) + \sum_{r=1}^{n} b_{2r}x_r, \text{ etc.}$$

The noise is assumed to be Gaussian in the remainder of this paper.

Assume the statistical characteristics of the noise are independent of time (i.e., stationary noise) over the sampling

interval, and that the autocorrelation of the noise $\phi(t)$ can be evaluated. Then (m_{rs}) is the inverse of

$$\begin{pmatrix} \overline{\eta^2} - \bar{\eta}^2 & \phi(\tau) - \bar{\eta}^2 & \phi(2\tau) - \bar{\eta}^2 & \cdots \\ \phi(\tau) - \bar{\eta}^2 & \overline{\eta^2} - \bar{\eta}^2 & \phi(\tau) - \bar{\eta}^2 & \\ \phi(2\tau) - \bar{\eta}^2 & \phi(\tau) - \bar{\eta}^2 & \ddots & \\ \vdots & & & \overline{\eta^2} - \bar{\eta}^2 \end{pmatrix},$$

where τ is the time between samples and $\overline{\eta^2}$ is second moment (or average power) of the noise.

If the noise spectrum has a sharp high-frequency cutoff, and if $1/\tau$ is twice this cutoff frequency, the procedure I_λ takes on a simple form. Consider the noise shifted by its average $\bar{\eta}$. If the noise has a spectrum of the form

$$G(\omega) = \begin{cases} G_o & 0 \le \omega \le \omega_o \\ 0 & \omega > \omega_o \end{cases},$$

where G_o is a constant, then the correlation function is

$$\begin{aligned} \phi(t) &= \int_o^\infty G(\omega) \cos \omega t \, d\omega \\ &= G_o \int_o^{\omega_o} \cos \omega t \, d\omega = G_o \frac{\sin \omega_o t}{t}, \end{aligned}$$

for $t > 0$ and $\phi(o) = G_o\omega_o$. If $1/\tau = 2(\omega_o/2\pi)$, $\phi(k\tau) = G_o\omega_o \dfrac{\sin k\pi}{k\pi} = 0$

for k = 1, 2, 3, ... In other words, the covariance matrix of the noise is diagonal and $m_{rs} = \left[\overline{\eta^2} - \bar{\eta}^2\right]^{-1}\delta_{rs}$. Hence I_λ reduces to a comparison of

$$\left[\overline{\eta^2} - \bar{\eta}^2\right]\log(w_1\lambda_1) - \frac{1}{2}\sum_{r=1}^{n}(u_{1r}+\bar{\eta})^2 + \sum_{r=1}^{n}(u_{1r}+\bar{\eta})x_r,$$

$$\left[\overline{\eta^2} - \bar{\eta}^2\right]\log(w_2\lambda_2) - \frac{1}{2}\sum_{r=1}^{n}(u_{2r}+\bar{\eta})^2 + \sum_{r=1}^{n}(u_{2r}+\bar{\eta})x_r, \text{ etc.}$$

IV. Probability of Correct Identification

Let E_{ij} be the set of x_i's such that

$$\{ c_i - c_j + \sum_{r=1}^{n} (b_{ir}-b_{jr})x_r \leq 0 \} .$$

Then $p_j(I_\lambda)$ is the probability of $E_{1j} \cap E_{2j} \cap E_{3j} \cap \cdots \cap E_{Nj}$ given the noisy waveform is the j-th standard waveform. Theoretically one can evaluate $p_j(I_\lambda)$ since the x_i's have a known multivariate normal density function. In practice it may be very difficult to evaluate $p_j(I_\lambda)$ for large N and n. If it is not practical to evaluate $p_j(I_\lambda)$ directly, one can use upper and lower bounds for $p_j(I_\lambda)$.

In analyzing a system the parameters of the system are given and $p_j(I_\lambda)$ must be determined. With a lower bound for $p_j(I_\lambda)$ one can make statements like--for the given parameter values the average probability of correct identification is at least .93. An upper bound for $p_j(I_\lambda)$ would be of little help in analyzing a given system. An upper bound is more helpful in design than in analysis. In design, $p_j(I_\lambda)$ is specified and the system parameters must be determined. With an upperbound for $p_j(I_\lambda)$ one can make statements like--to achieve the specified value of $p_j(I_\lambda)$ one must take at least 31 samples from each input waveform. On the other hand, with a lower bound for $p_j(I_\lambda)$ one can make statements like--to achieve the specified value of $p_j(I_\lambda)$ it is not necessary to take more than 43 samples from each input waveform. A lower bound will result in over designing and an upper bound will result in under designing the system.

The probability of E_{ij} given the noisy waveform is the j-th standard waveform is an upper bound for $p_j(I_\lambda)$ for all values of i. One can select i to minimize this bound; in other words, the "best" upper bound is

$$\min\{\Pr(E_{1j}|\text{j-th stand.}),\ \Pr(E_{2j}|\text{j-th stand.}),\ \ldots.,\ \Pr(E_{Nj}|\text{j-th stand.})\}.$$

This bound is easy to evaluate. The probability of E_{ij} given the noisy waveform is the j-th standard waveform is equal to the probability that

$$\sum_{r=1}^{n}(b_{ir}-b_{jr})(x_r-u_{jr}-\bar{\eta}) \leq c_j - c_i - \sum_{r=1}^{n}(b_{ir}-b_{jr})(u_{jr}+\bar{\eta}).$$

The left-hand side of this inequality is a normal random variable with mean zero and variance

$$\sum_{r=1}^{n}\sum_{s=1}^{n}(b_{ir}-b_{jr})(b_{is}-b_{js})\left[\phi(|r-s|\tau) - \bar{\eta}^2\right]$$

Hence $\Pr(E_{ij}|\text{j-th stand.})$ equals the probability a normal random variable with zero mean and unit variance is less than

$$\left[c_j - c_i - \sum_{r=1}^{n}(b_{ir} - b_{jr})(u_{jr} + \bar{\eta})\right] \cdot \left[\sum_{r=1}^{n}\sum_{s=1}^{n}(b_{ir} - b_{jr})(b_{is} - b_{js})\left[\phi(|r-s|\tau) - \bar{\eta}^2\right]\right]^{-1/2}.$$

Let K_{ij} represent this constant. Since K_{ij} gives an upper bound for all values of i, the "best" upper bound is obtained when i minimizes K_{ij}. If the noise spectrum has a sharp high-frequency cutoff, and if $1/\tau$ is twice this cutoff frequency,

$$K_{ij} = \frac{1}{\sqrt{n\rho_{ij}}} \log \left[\frac{w_j \lambda_j}{w_i \lambda_i} \right] + \frac{1}{2} \sqrt{n\rho_{ij}} \quad ,$$

$$\text{where } \rho_{ij} = \frac{1}{n} \sum_{r=1}^{n} (u_{jr} - u_{ir})^2 \Big/ \left[\overline{\eta^2} - \bar{\eta}^2 \right] \quad .$$

Note that ρ_{ij} is the ratio of the mean square deviation between u_{jr} and u_{ir} to the expected square deviation of the noise from its mean. In Figure 1, $\Pr(E_{ij} \mid j\text{-th stand.})$ is graphed against n and ρ_{ij} for $w_i\lambda_i = w_j\lambda_j$. If $w_i\lambda_i = w_j\lambda_j$ for all i, then the value of i that minimizes ρ_{ij} will minimize K_{ij}.

The probability of $E_{ij} \cap E_{kj}$ given the noisy waveform is the j-th standard waveform is also an upper bound for $p_j(I_\lambda)$. This bound is smaller than the bound derived above, but it is also more difficult to evaluate. The probability of $E_{ij} \cap E_{kj}$ can be evaluated by transforming the random variables to a standard form and using tabulated values of the bivariate normal distribution.

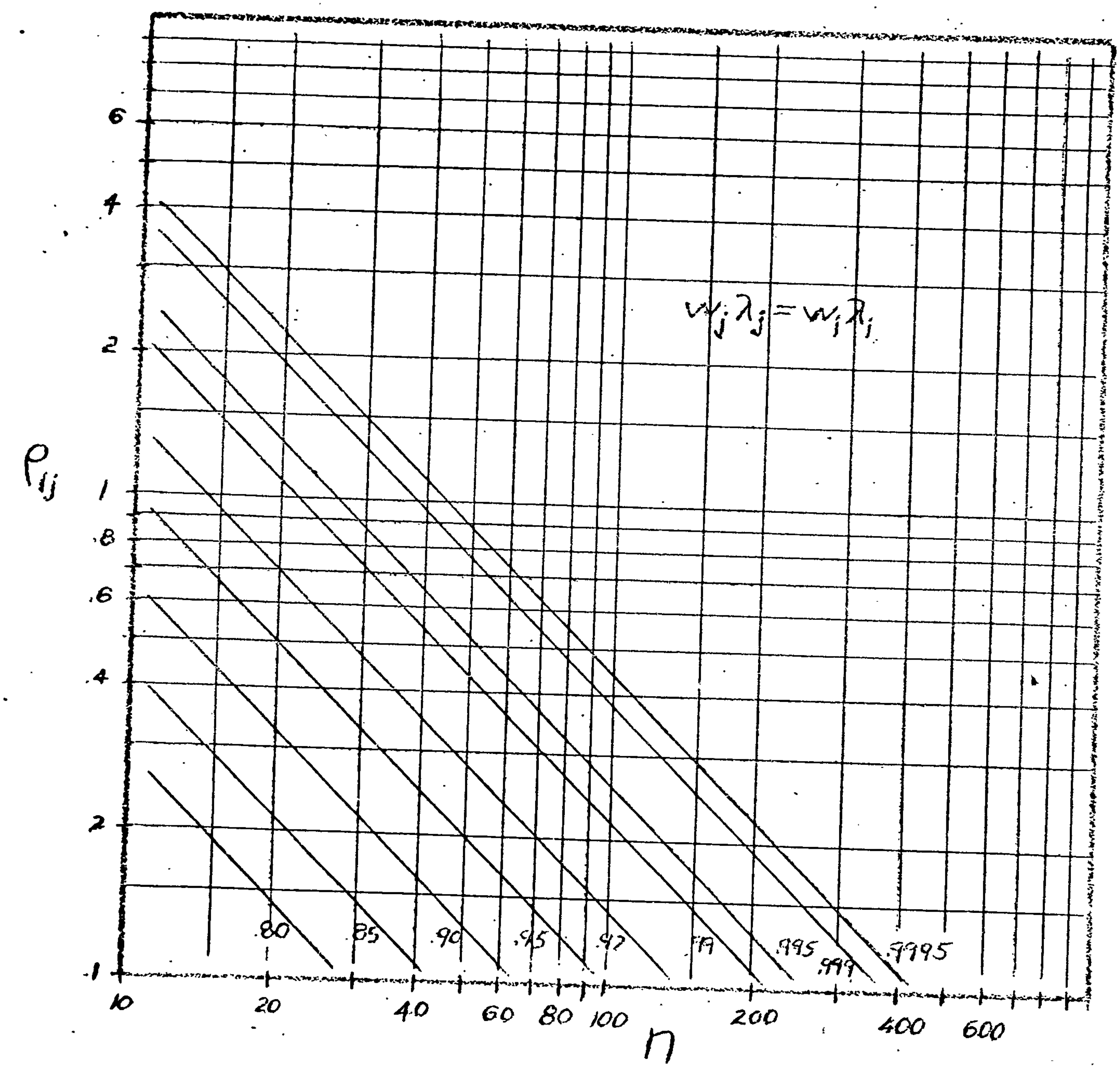

Figure 1. Graph of $Pr(E_{ij} \mid j\text{-th stand.})$

V. Preliminary Rejection

If the number of standard waveforms N is large, it is awkward to select the value of i that maximizes $c_i + \sum_{r=1}^{n} b_{ir}x_r$. The selection can be simplified with preliminary rejection of non-contenders. If $c_1 + \sum_{r=1}^{n} b_{1r}x_r$ is less than a fixed threshold t_1, it is not compared to $c_2 + \sum_{r=1}^{n} b_{2r}x_r, c_3 + \sum_{r=1}^{n} b_{3r}x_r$, etc. It is easy to evaluate the probability that the j-th waveform will be rejected erroneously, i.e.,

$$\Pr\left\{ c_j + \sum_{r=1}^{n} b_{jr}x_r < t_j \;\middle|\; \text{j-th type} \right\} .$$

The threshold t_j is selected so that probability of errnoneous rejection is "sufficiently" small.